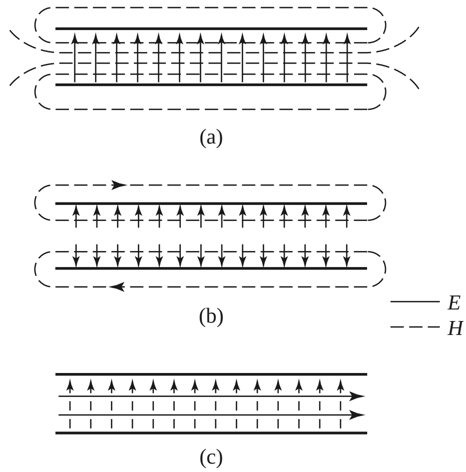

FIGURE 3.5 Field lines for the (a) TEM, (b) TM_1, and (c) TE_1 modes of a parallel plate waveguide. There is no variation across the width of the waveguide.

3.3 RECTANGULAR WAVEGUIDE

Rectangular waveguides were one of the earliest types of transmission lines used to transport microwave signals, and they are still used for many applications. A large variety of components such as couplers, detectors, isolators, attenuators, and slotted lines are commercially available for various standard waveguide bands from 1 to 220 GHz. Figure 3.6 shows some of the standard rectangular waveguide components that are available. Because of the trend toward miniaturization and integration, most modern microwave circuitry is fabricated using planar transmission lines such as microstrips and stripline rather than waveguides. There is, however, still a need for waveguides in many cases, including high-power systems, millimeter wave applications, satellite systems, and some precision test applications.

The hollow rectangular waveguide can propagate TM and TE modes but not TEM waves since only one conductor is present. We will see that the TM and TE modes of a rectangular waveguide have cutoff frequencies below which propagation is not possible, similar to the TM and TE modes of the parallel plate guide.

TE Modes

The geometry of a rectangular waveguide is shown in Figure 3.7, where it is assumed that the guide is filled with a material of permittivity ϵ and permeability μ. It is standard convention to have the longest side of the waveguide along the x-axis, so that $a > b$.

TE waveguide modes are characterized by fields with $E_z = 0$, while H_z must satisfy the reduced wave equation of (3.21):

$$\left(\frac{\partial^2}{\partial x^2} + \frac{\partial^2}{\partial y^2} + k_c^2 \right) h_z(x, y) = 0, \tag{3.73}$$

with $H_z(x, y, z) = h_z(x, y)e^{-j\beta z}$; here $k_c = \sqrt{k^2 - \beta^2}$ is the cutoff wave number. The partial differential equation (3.73) can be solved by the method of separation of variables by letting

$$h_z(x, y) = X(x)Y(y) \tag{3.74}$$

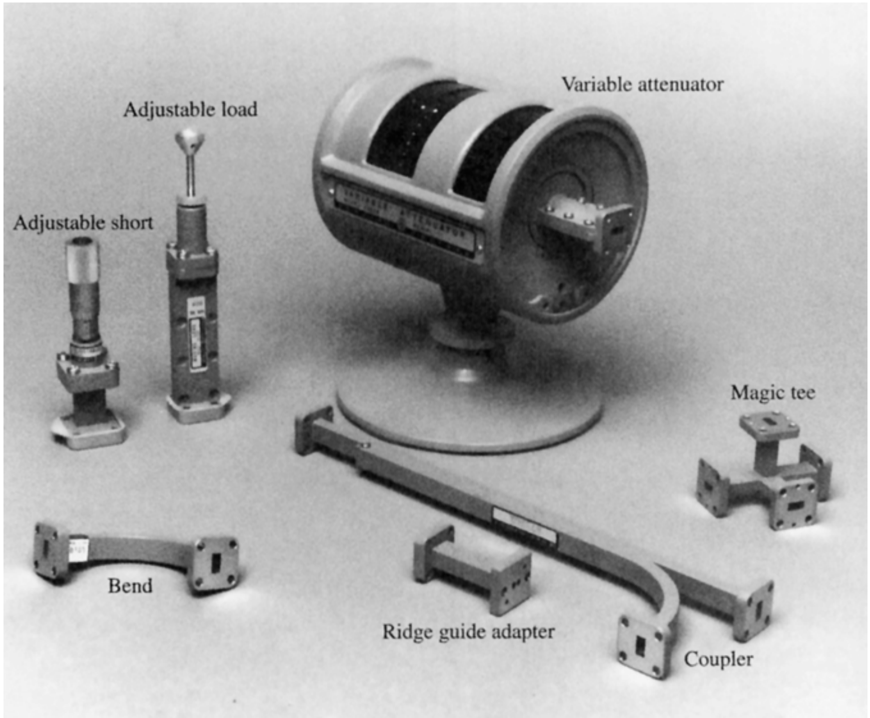

FIGURE 3.6 Photograph of Ka-band (WR-28) rectangular waveguide components. Clockwise from top: a variable attenuator, an E-H (magic) tee junction, a directional coupler, an adaptor to ridge waveguide, an E-plane swept bend, an adjustable short, and a sliding matched load.

and substituting into (3.73) to obtain

$$\frac{1}{X}\frac{d^2X}{dx^2} + \frac{1}{Y}\frac{d^2Y}{dy^2} + k_c^2 = 0. \tag{3.75}$$

Then, by the usual separation-of-variables argument (see Section 1.5), each of the terms in (3.75) must be equal to a constant, so we define separation constants k_x and k_y such that

$$\frac{d^2X}{dx^2} + k_x^2 X = 0, \tag{3.76a}$$

$$\frac{d^2Y}{dy^2} + k_y^2 Y = 0, \tag{3.76b}$$

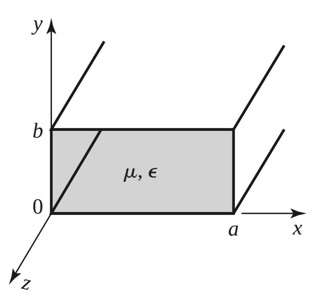

FIGURE 3.7 Geometry of a rectangular waveguide.

and

$$k_x^2 + k_y^2 = k_c^2. \tag{3.77}$$

The general solution for h_z can then be written as

$$h_z(x, y) = (A \cos k_x x + B \sin k_x x)(C \cos k_y y + D \sin k_y y). \tag{3.78}$$

To evaluate the constants in (3.78) we must apply the boundary conditions on the electric field components tangential to the waveguide walls. That is,

$$e_x(x, y) = 0, \qquad \text{at } y = 0, b, \tag{3.79a}$$

$$e_y(x, y) = 0, \qquad \text{at } x = 0, a. \tag{3.79b}$$

We therefore cannot use h_z of (3.78) directly but must first use (3.19c) and (3.19d) to find e_x and e_y from h_z:

$$e_x = \frac{-j\omega\mu}{k_c^2} k_y (A \cos k_x x + B \sin k_x x)(-C \sin k_y y + D \cos k_y y), \tag{3.80a}$$

$$e_y = \frac{j\omega\mu}{k_c^2} k_x (-A \sin k_x x + B \cos k_x x)(C \cos k_y y + D \sin k_y y). \tag{3.80b}$$

Then from (3.79a) and (3.80a) we see that $D = 0$, and $k_y = n\pi/b$ for $n = 0, 1, 2\ldots$. From (3.79b) and (3.80b) we have that $B = 0$ and $k_x = m\pi/a$ for $m = 0, 1, 2\ldots$. The final solution for H_z is then

$$H_z(x, y, z) = A_{mn} \cos \frac{m\pi x}{a} \cos \frac{n\pi y}{b} e^{-j\beta z}, \tag{3.81}$$

where A_{mn} is an arbitrary amplitude constant composed of the remaining constants A and C of (3.78).

The transverse field components of the TE_{mn} mode can be found using (3.19) and (3.81):

$$E_x = \frac{j\omega\mu n\pi}{k_c^2 b} A_{mn} \cos \frac{m\pi x}{a} \sin \frac{n\pi y}{b} e^{-j\beta z}, \tag{3.82a}$$

$$E_y = \frac{-j\omega\mu m\pi}{k_c^2 a} A_{mn} \sin \frac{m\pi x}{a} \cos \frac{n\pi y}{b} e^{-j\beta z}, \tag{3.82b}$$

$$H_x = \frac{j\beta m\pi}{k_c^2 a} A_{mn} \sin \frac{m\pi x}{a} \cos \frac{n\pi y}{b} e^{-j\beta z}, \tag{3.82c}$$

$$H_y = \frac{j\beta n\pi}{k_c^2 b} A_{mn} \cos \frac{m\pi x}{a} \sin \frac{n\pi y}{b} e^{-j\beta z}. \tag{3.82d}$$

The propagation constant is

$$\beta = \sqrt{k^2 - k_c^2} = \sqrt{k^2 - \left(\frac{m\pi}{a}\right)^2 - \left(\frac{n\pi}{b}\right)^2}, \tag{3.83}$$

which is seen to be real, corresponding to a propagating mode, when

$$k > k_c = \sqrt{\left(\frac{m\pi}{a}\right)^2 + \left(\frac{n\pi}{b}\right)^2}.$$

Each mode (each combination of m and n) has a cutoff frequency $f_{c_{mn}}$ given by

$$f_{c_{mn}} = \frac{k_c}{2\pi\sqrt{\mu\epsilon}} = \frac{1}{2\pi\sqrt{\mu\epsilon}}\sqrt{\left(\frac{m\pi}{a}\right)^2 + \left(\frac{n\pi}{b}\right)^2}. \tag{3.84}$$

The mode with the lowest cutoff frequency is called the dominant mode; because we have assumed $a > b$, the lowest cutoff frequency occurs for the $\mathrm{TE}_{10}(m = 1,\ n = 0)$ mode:

$$f_{c_{10}} = \frac{1}{2a\sqrt{\mu\epsilon}}. \tag{3.85}$$

Thus the TE_{10} mode is the dominant TE mode and, as we will see, the overall dominant mode of the rectangular waveguide. Observe that the field expressions for $\bar{E}$ and $\bar{H}$ in (3.82) are all zero if both $m = n = 0$; there is no TE_{00} mode.

At a given operating frequency f only those modes having $f > f_c$ will propagate; modes with $f < f_c$ will lead to an imaginary β (or real α), meaning that all field components will decay exponentially away from the source of excitation. Such modes are referred to as *cutoff modes*, or *evanescent modes*. If more than one mode is propagating, the waveguide is said to be *overmoded*.

From (3.22) the wave impedance that relates the transverse electric and magnetic fields is

$$Z_{\mathrm{TE}} = \frac{E_x}{H_y} = \frac{-E_y}{H_x} = \frac{k\eta}{\beta}, \tag{3.86}$$

where $\eta = \sqrt{\mu/\epsilon}$ is the intrinsic impedance of the material filling the waveguide. Note that Z_{TE} is real when β is real (a propagating mode) but is imaginary when β is imaginary (a cutoff mode).

The guide wavelength is defined as the distance between two equal-phase planes along the waveguide and is equal to

$$\lambda_g = \frac{2\pi}{\beta} > \frac{2\pi}{k} = \lambda, \tag{3.87}$$

which is thus greater than λ, the wavelength of a plane wave in the medium filling the guide. The phase velocity is

$$v_p = \frac{\omega}{\beta} > \frac{\omega}{k} = 1/\sqrt{\mu\epsilon}, \tag{3.88}$$

which is greater than $1/\sqrt{\mu\epsilon}$, the speed of light (plane wave) in the medium.

In the vast majority of waveguide applications the operating frequency and guide dimensions are chosen so that only the dominant TE_{10} mode will propagate. Because of the practical importance of the TE_{10} mode, we will list the field components and derive the attenuation due to conductor loss for this case.

Specializing (3.81) and (3.82) to the $m = 1,\ n = 0$ case gives the following results for the TE_{10} mode fields:

$$H_z = A_{10}\cos\frac{\pi x}{a}e^{-j\beta z}, \tag{3.89a}$$

$$E_y = \frac{-j\omega\mu a}{\pi}A_{10}\sin\frac{\pi x}{a}e^{-j\beta z}, \tag{3.89b}$$

$$H_x = \frac{j\beta a}{\pi}A_{10}\sin\frac{\pi x}{a}e^{-j\beta z}, \tag{3.89c}$$

$$E_x = E_z = H_y = 0. \tag{3.89d}$$

The cutoff wave number and propagation constant for the TE_{10} mode are, respectively,

$$k_c = \pi/a, \tag{3.90}$$

$$\beta = \sqrt{k^2 - (\pi/a)^2}. \tag{3.91}$$

The power flow down the guide for the TE_{10} mode can be calculated as

$$\begin{aligned} P_{10} &= \frac{1}{2}\mathrm{Re}\int_{x=0}^{a}\int_{y=0}^{b} \bar{E} \times \bar{H}^* \cdot \hat{z}\, dy\, dx \\ &= \frac{1}{2}\mathrm{Re}\int_{x=0}^{a}\int_{y=0}^{b} E_y H_x^*\, dy\, dx \\ &= \frac{\omega\mu a^2}{2\pi^2}\mathrm{Re}(\beta)|A_{10}|^2 \int_{x=0}^{a}\int_{y=0}^{b} \sin^2\frac{\pi x}{a}\, dy\, dx \\ &= \frac{\omega\mu a^3|A_{10}|^2 b}{4\pi^2}\mathrm{Re}(\beta). \end{aligned} \tag{3.92}$$

Note that this result gives nonzero real power only when β is real, corresponding to a propagating mode.

Attenuation in a rectangular waveguide may occur due to dielectric loss or conductor loss. Dielectric loss can be treated by making ϵ complex and using the general result given in (3.29). Conductor loss is best treated using the perturbation method. The power lost per unit length due to finite wall conductivity is, from (1.131),

$$P_\ell = \frac{R_s}{2}\int_C |\bar{J}_s|^2 d\ell, \tag{3.93}$$

where R_s is the wall surface resistance, and the integration contour C encloses the inside perimeter of the guide walls. There are surface currents on all four walls, but from symmetry the currents on the top and bottom walls are identical, as are the currents on the left and right side walls. So we can compute the power lost in the walls at $x = 0$ and $y = 0$ and double their sum to obtain the total power loss. The surface current on the $x = 0$ (left) wall is

$$\bar{J}_s = \hat{n} \times \bar{H}|_{x=0} = \hat{x} \times \hat{z}H_z|_{x=0} = -\hat{y}H_z|_{x=0} = -\hat{y}A_{10}e^{-j\beta z}, \tag{3.94a}$$

and the surface current on the $y = 0$ (bottom) wall is

$$\begin{aligned} \bar{J}_s &= \hat{n} \times \bar{H}|_{y=0} = \hat{y} \times (\hat{x}H_x|_{y=0} + \hat{z}H_z|_{y=0}) \\ &= -\hat{z}\frac{j\beta a}{\pi}A_{10}\sin\frac{\pi x}{a}e^{-j\beta z} + \hat{x}A_{10}\cos\frac{\pi x}{a}e^{-j\beta z}. \end{aligned} \tag{3.94b}$$

Substituting (3.94) into (3.93) gives

$$\begin{aligned} P_\ell &= R_s\int_{y=0}^{b}|J_{sy}|^2 dy + R_s\int_{x=0}^{a}\left[|J_{sx}|^2 + |J_{sz}|^2\right] dx \\ &= R_s|A_{10}|^2\left(b + \frac{a}{2} + \frac{\beta^2 a^3}{2\pi^2}\right). \end{aligned} \tag{3.95}$$

The attenuation due to conductor loss for the TE_{10} mode is then

$$\alpha_c = \frac{P_\ell}{2P_{10}} = \frac{2\pi^2 R_s(b + a/2 + \beta^2 a^3/2\pi^2)}{\omega\mu a^3 b\beta}$$
$$= \frac{R_s}{a^3 b\beta k\eta}(2b\pi^2 + a^3k^2) \text{ Np/m.} \tag{3.96}$$

TM Modes

TM modes are characterized by fields with $H_z = 0$, while E_z must satisfy the reduced wave equation (3.25):

$$\left(\frac{\partial^2}{\partial x^2} + \frac{\partial^2}{\partial y^2} + k_c^2\right) e_z(x, y) = 0, \tag{3.97}$$

with $E_z(x, y, z) = e_z(x, y)e^{-j\beta z}$ and $k_c^2 = k^2 - \beta^2$. Equation (3.97) can be solved by the separation-of-variables procedure that was used for TE modes. The general solution is

$$e_z(x, y) = (A\cos k_x x + B\sin k_x x)(C\cos k_y y + D\sin k_y y). \tag{3.98}$$

The boundary conditions can be applied directly to e_z:

$$e_z(x, y) = 0, \qquad \text{at } x = 0, a, \tag{3.99a}$$
$$e_z(x, y) = 0, \qquad \text{at } y = 0, b. \tag{3.99b}$$

We will see that satisfaction of these conditions on e_z will lead to satisfaction of the boundary conditions by e_x and e_y.

Applying (3.99a) to (3.98) shows that $A = 0$ and $k_x = m\pi/a$ for $m = 1, 2, 3\ldots$. Similarly, applying (3.99b) to (3.98) shows that $C = 0$ and $k_y = n\pi/b$ for $n = 1, 2, 3\ldots$. The solution for E_z then reduces to

$$E_z(x, y, z) = B_{mn}\sin\frac{m\pi x}{a}\sin\frac{n\pi y}{b}e^{-j\beta z}, \tag{3.100}$$

where B_{mn} is an arbitrary amplitude constant.

The transverse field components for the TM_{mn} mode can be computed from (3.23) and (3.100) as

$$E_x = \frac{-j\beta m\pi}{ak_c^2}B_{mn}\cos\frac{m\pi x}{a}\sin\frac{n\pi y}{b}e^{-j\beta z}, \tag{3.101a}$$
$$E_y = \frac{-j\beta n\pi}{bk_c^2}B_{mn}\sin\frac{m\pi x}{a}\cos\frac{n\pi y}{b}e^{-j\beta z}, \tag{3.101b}$$
$$H_x = \frac{j\omega\epsilon n\pi}{bk_c^2}B_{mn}\sin\frac{m\pi x}{a}\cos\frac{n\pi y}{b}e^{-j\beta z}, \tag{3.101c}$$
$$H_y = \frac{-j\omega\epsilon m\pi}{ak_c^2}B_{mn}\cos\frac{m\pi x}{a}\sin\frac{n\pi y}{b}e^{-j\beta z}. \tag{3.101d}$$

As for the TE modes, the propagation constant is

$$\beta = \sqrt{k^2 - k_c^2} = \sqrt{k^2 - \left(\frac{m\pi}{a}\right)^2 - \left(\frac{n\pi}{b}\right)^2} \tag{3.102}$$

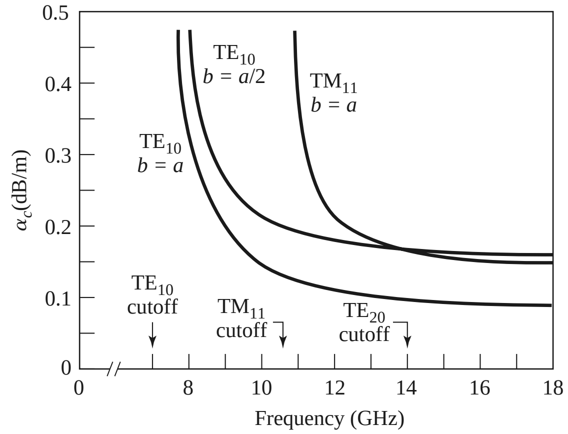

FIGURE 3.8 Attenuation of various modes in a rectangular brass waveguide with $a = 2.0$ cm.

and is real for propagating modes and imaginary for cutoff modes. The cutoff frequencies for the TM_{mn} modes are also the same as those of the TE_{mn} modes, as given in (3.84). The guide wavelength and phase velocity for TM modes are also the same as those for TE modes.

Observe that the field expressions for $\bar{E}$ and $\bar{H}$ in (3.101) are identically zero if either m or n is zero. Thus there is no TM_{00}, TM_{01}, or TM_{10} mode, and the lowest order TM mode to propagate (lowest f_c) is the TM_{11} mode, having a cutoff frequency of

$$f_{c_{11}} = \frac{1}{2\pi\sqrt{\mu\epsilon}}\sqrt{\left(\frac{\pi}{a}\right)^2 + \left(\frac{\pi}{b}\right)^2}, \tag{3.103}$$

which is seen to be larger than $f_{c_{10}}$, the cutoff frequency of the TE_{10} mode.

The wave impedance relating the transverse electric and magnetic fields for TM modes is, from (3.26),

$$Z_{\text{TM}} = \frac{E_x}{H_y} = \frac{-E_y}{H_x} = \frac{\beta\eta}{k}. \tag{3.104}$$

Attenuation due to dielectric loss is computed in the same way as for TE modes, with the same result. The calculation of attenuation due to conductor loss is left as a problem; Figure 3.8 shows attenuation versus frequency for some TE and TM modes in a rectangular waveguide. Table 3.2 summarizes results for TE and TM wave propagation in rectangular waveguides, and Figure 3.9 shows the field lines for several of the lowest order TE and TM modes.

EXAMPLE 3.1 CHARACTERISTICS OF A RECTANGULAR WAVEGUIDE

Consider a length of Teflon-filled, copper K-band rectangular waveguide having dimensions $a = 1.07$ cm and $b = 0.43$ cm. Find the cutoff frequencies of the first five propagating modes. If the operating frequency is 15 GHz, find the attenuation due to dielectric and conductor losses.

TABLE 3.2 Summary of Results for Rectangular Waveguide

Quantity	TE_{mn} Mode	TM_{mn} Mode
k	$\omega\sqrt{\mu\epsilon}$	$\omega\sqrt{\mu\epsilon}$
k_c	$\sqrt{(m\pi/a)^2 + (n\pi/b)^2}$	$\sqrt{(m\pi/a)^2 + (n\pi/b)^2}$
β	$\sqrt{k^2 - k_c^2}$	$\sqrt{k^2 - k_c^2}$
λ_c	$\dfrac{2\pi}{k_c}$	$\dfrac{2\pi}{k_c}$
λ_g	$\dfrac{2\pi}{\beta}$	$\dfrac{2\pi}{\beta}$
v_p	$\dfrac{\omega}{\beta}$	$\dfrac{\omega}{\beta}$
α_d	$\dfrac{k^2 \tan\delta}{2\beta}$	$\dfrac{k^2 \tan\delta}{2\beta}$
E_z	0	$B \sin\dfrac{m\pi x}{a} \sin\dfrac{n\pi y}{b} e^{-j\beta z}$
H_z	$A \cos\dfrac{m\pi x}{a} \cos\dfrac{n\pi y}{b} e^{-j\beta z}$	0
E_x	$\dfrac{j\omega\mu n\pi}{k_c^2 b} A \cos\dfrac{m\pi x}{a} \sin\dfrac{n\pi y}{b} e^{-j\beta z}$	$\dfrac{-j\beta m\pi}{k_c^2 a} B \cos\dfrac{m\pi x}{a} \sin\dfrac{n\pi y}{b} e^{-j\beta z}$
E_y	$\dfrac{-j\omega\mu m\pi}{k_c^2 a} A \sin\dfrac{m\pi x}{a} \cos\dfrac{n\pi y}{b} e^{-j\beta z}$	$\dfrac{-j\beta n\pi}{k_c^2 b} B \sin\dfrac{m\pi x}{a} \cos\dfrac{n\pi y}{b} e^{-j\beta z}$
H_x	$\dfrac{j\beta m\pi}{k_c^2 a} A \sin\dfrac{m\pi x}{a} \cos\dfrac{n\pi y}{b} e^{-j\beta z}$	$\dfrac{j\omega\epsilon n\pi}{k_c^2 b} B \sin\dfrac{m\pi x}{a} \cos\dfrac{n\pi y}{b} e^{-j\beta z}$
H_y	$\dfrac{j\beta n\pi}{k_c^2 b} A \cos\dfrac{m\pi x}{a} \sin\dfrac{n\pi y}{b} e^{-j\beta z}$	$\dfrac{-j\omega\epsilon m\pi}{k_c^2 a} B \cos\dfrac{m\pi x}{a} \sin\dfrac{n\pi y}{b} e^{-j\beta z}$
Z	$Z_{\text{TE}} = \dfrac{k\eta}{\beta}$	$Z_{\text{TM}} = \dfrac{\beta\eta}{k}$

Solution

From Appendix G, for Teflon, $\epsilon_r = 2.08$ and $\tan\delta = 0.0004$. From (3.84) the cutoff frequencies are given by

$$f_{c_{mn}} = \frac{c}{2\pi\sqrt{\epsilon_r}}\sqrt{\left(\frac{m\pi}{a}\right)^2 + \left(\frac{n\pi}{b}\right)^2}.$$

Computing f_c for the first few values of m and n gives the following results:

Mode	m	n	f_c(GHz)
TE	1	0	9.72
TE	2	0	19.44
TE	0	1	24.19
TE, TM	1	1	26.07
TE, TM	2	1	31.03

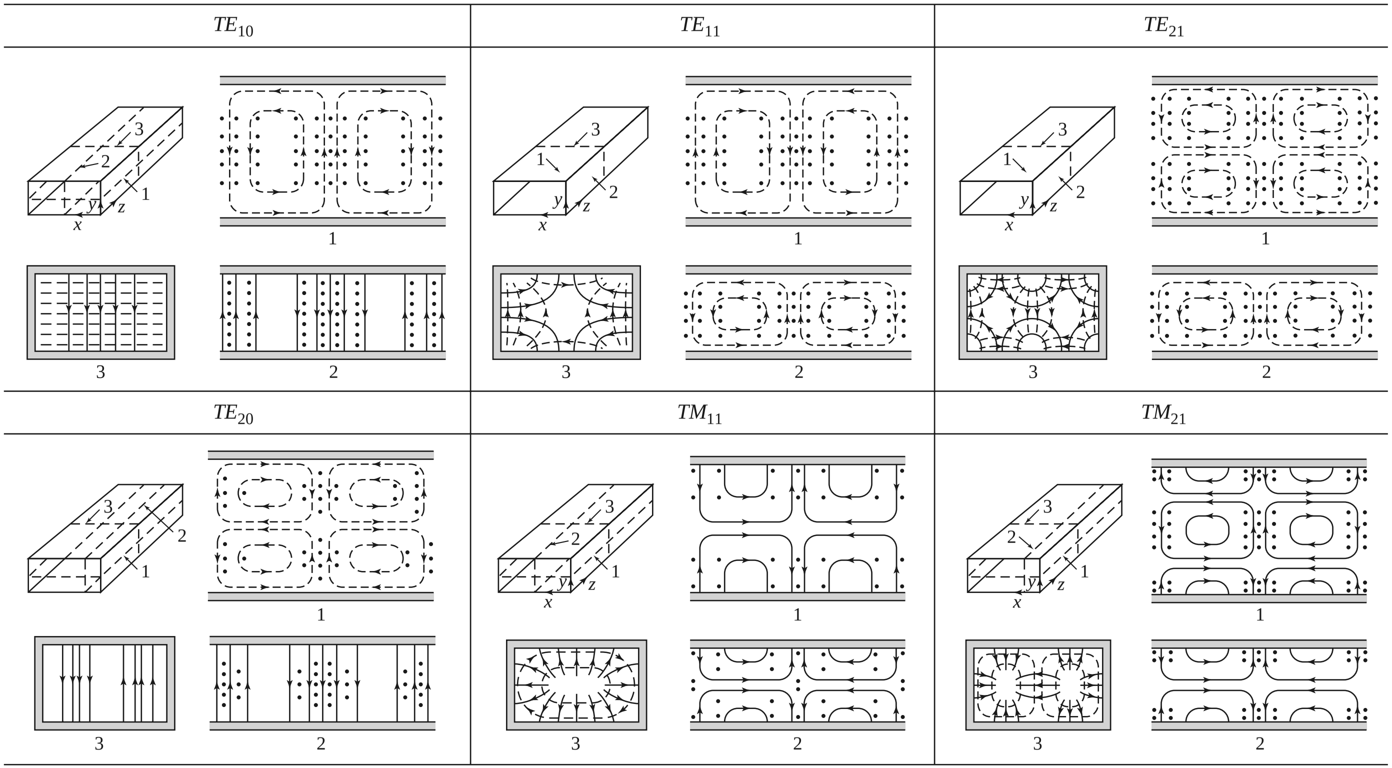

FIGURE 3.9 Field lines for some of the lower order modes of a rectangular waveguide.

Reprinted with permission from S. Ramo, J. R. Whinnery, and T. Van Duzer, *Fields and Waves in Communication Electronics*. Copyright © 1965 by John Wiley & Sons, Inc. Table 8.02.

Thus the TE_{10}, TE_{20}, TE_{01}, TE_{11}, and TM_{11} modes will be the first five modes to propagate.

At 15 GHz, $k = 453.1\ \text{m}^{-1}$, and the propagation constant for the TE_{10} mode is

$$\beta = \sqrt{\left(\frac{2\pi f\sqrt{\epsilon_r}}{c}\right)^2 - \left(\frac{\pi}{a}\right)^2} = \sqrt{k^2 - \left(\frac{\pi}{a}\right)^2} = 345.1\ \text{m}^{-1}.$$

From (3.29), the attenuation due to dielectric loss is

$$\alpha_d = \frac{k^2 \tan\delta}{2\beta} = 0.119\ \text{Np/m} = 1.03\ \text{dB/m}.$$

The surface resistivity of the copper walls is ($\sigma = 5.8 \times 10^7$ S/m)

$$R_s = \sqrt{\frac{\omega\mu_0}{2\sigma}} = 0.032\ \Omega,$$

and the attenuation due to conductor loss, from (3.96), is

$$\alpha_c = \frac{R_s}{a^3 b\beta k\eta}(2b\pi^2 + a^3k^2) = 0.050\ \text{Np/m} = 0.434\ \text{dB/m}.$$

■

TE_{m0} Modes of a Partially Loaded Waveguide

The above results apply to an empty waveguide as well as one filled with a homogeneous dielectric or magnetic material, but in some cases of practical interest (such as impedance matching or phase-shifting sections) a waveguide is used with a partial dielectric filling. In this case an additional set of boundary conditions are introduced at the material interface, necessitating a new analysis. To illustrate the technique we will consider the TE_{m0} modes of a rectangular waveguide that is partially filled with a dielectric slab, as shown in Figure 3.10. The analysis still follows the basic procedure outlined at the end of Section 3.1.

Since the geometry is uniform in the y direction and $n = 0$, the TE_{m0} modes have no y dependence. Then the wave equation of (3.21) for h_z can be written separately for the dielectric and air regions as

$$\left(\frac{\partial^2}{\partial x^2} + k_d^2\right)h_z = 0, \qquad \text{for } 0 \le x \le t, \tag{3.105a}$$

$$\left(\frac{\partial^2}{\partial x^2} + k_a^2\right)h_z = 0, \qquad \text{for } t \le x \le a, \tag{3.105b}$$

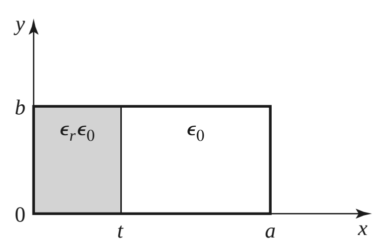

FIGURE 3.10 Geometry of a partially loaded rectangular waveguide.

where k_d and k_a are the cutoff wave numbers for the dielectric and air regions, defined as follows:

$$\beta = \sqrt{\epsilon_r k_0^2 - k_d^2}, \tag{3.106a}$$

$$\beta = \sqrt{k_0^2 - k_a^2}. \tag{3.106b}$$

These relations incorporate the fact that the propagation constant, β, must be the same in both regions to ensure phase matching (see Section 1.8) of the fields along the interface at x = t. The solutions to (3.105) can be written as

$$h_z = \begin{cases} A \cos k_d x + B \sin k_d x & \text{for } 0 \le x \le t \\ C \cos k_a(a - x) + D \sin k_a(a - x) & \text{for } t \le x \le a, \end{cases} \tag{3.107}$$

where the form of the solution for $t < x < a$ was chosen to simplify the evaluation of boundary conditions at $x = a$.

We need $\hat{y}$ and $\hat{z}$ electric and magnetic field components to apply the boundary conditions at $x = 0,\ t$, and a. $E_z = 0$ for TE modes, and $H_y = 0$ since $\partial/\partial y = 0$. E_y is found from (3.19d) as

$$e_y = \begin{cases} \dfrac{j\omega\mu_0}{k_d}(-A \sin k_d x + B \cos k_d x) & \text{for } 0 \le x \le t \\ \dfrac{j\omega\mu_0}{k_a}[C \sin k_a(a - x) - D \cos k_a(a - x)] & \text{for } t \le x \le a. \end{cases} \tag{3.108}$$

To satisfy the boundary conditions that $E_y = 0$ at $x = 0$ and $x = a$ requires that $B = D = 0$. We next enforce continuity of tangential fields $(E_y,\ H_z)$ at $x = t$. Equations (3.107) and (3.108) then give the following:

$$\frac{-A}{k_d} \sin k_d t = \frac{C}{k_a} \sin k_a(a - t),$$

$$A \cos k_d t = C \cos k_a(a - t).$$

Because this is a homogeneous set of equations, the determinant must vanish in order to have a nontrivial solution. Thus,

$$k_a \tan k_d t + k_d \tan k_a(a - t) = 0. \tag{3.109}$$

Using (3.106) allows k_a and k_d to be expressed in terms of β, so (3.109) can be solved numerically for β. There is an infinite number of solutions to (3.109), corresponding to the propagation constants of the TE_{m0} modes.

This technique can be applied to many other waveguide geometries involving dielectric or magnetic material inhomogeneities, such as the surface waveguide of Section 3.6 or the ferrite-loaded waveguide of Section 9.3. In some cases, however, it will be impossible to satisfy all the necessary boundary conditions with only TE- or TM-type modes, and a hybrid combination of both types of modes may be required.

POINT OF INTEREST: Waveguide Flanges

There are two commonly used waveguide flanges: the cover flange and the choke flange. As shown in the accompanying figure, two waveguides with cover-type flanges can be bolted together to form a contacting joint. To avoid reflections and resistive loss at this joint it is necessary that the contacting surfaces be smooth, clean, and square because RF currents must flow across this discontinuity. In high-power applications voltage breakdown may occur at an imperfect junction. Otherwise, the simplicity of the cover-to-cover connection makes it preferable for general use. The SWR from such a joint is typically less than 1.03.

An alternative waveguide connection uses a cover flange against a choke flange, as shown in the figure. The choke flange is machined to form an effective radial transmission line in the narrow gap between the two flanges; this line is approximately $\lambda_g/4$ in length between the guide and the point of contact for the two flanges. Another $\lambda_g/4$ line is formed by a circular axial groove in the choke flange. Then the short circuit at the right-hand end of this groove is transformed into an open circuit at the contact point of the flanges. Any resistance in this contact is in series with an infinite (or very high) impedance and thus has little effect. This high impedance is transformed back into a short circuit (or very low impedance) at the edges of the waveguides to provide an effective low-resistance path for current flow across the joint. Because there is a negligible voltage drop across the ohmic contact between the flanges, voltage breakdown is avoided. Thus, the cover-to-choke connection can be useful for high-power applications. The SWR for this joint is typically less than 1.05 but is more frequency dependent than that of the cover-to-cover joint.

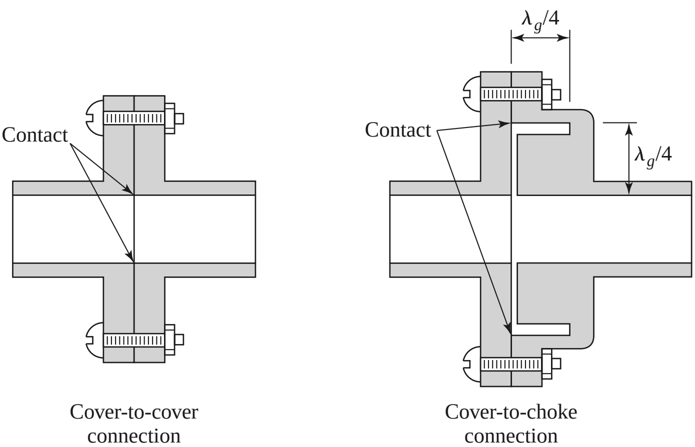

Reference: C. G. Montgomery, R. H. Dicke, and E. M. Purcell, *Principles of Microwave Circuits*, McGraw-Hill, New York, 1948.

3.4 CIRCULAR WAVEGUIDE

A hollow, round metal pipe also supports TE and TM waveguide modes. Figure 3.11 shows the geometry of such a circular waveguide, with inner radius a. Because cylindrical geometry is involved, it is appropriate to employ cylindrical coordinates. As in the rectangular

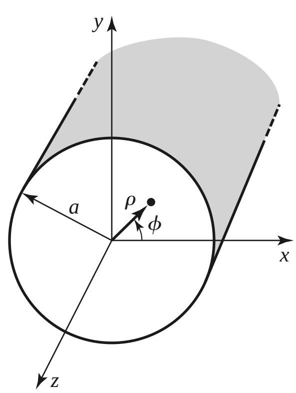

FIGURE 3.11 Geometry of a circular waveguide.